Activation of Wnt/β-catenin pathway mitigates blood–brain barrier dysfunction in Alzheimer's disease

Qi Wang,[1,2,†] Xiaomin Huang,[1,†] Yixun Su,[1,2] Guowei Yin,[1] Shouyu Wang,[2] Bin Yu,[2] Hui Li,[1,2] Junhua Qi,[1] Hui Chen,[3] Wen Zeng,[4] Kai Zhang,[5] Alexei Verkhratsky,[6,7] Jianqin Niu[2] and Chenju Yi[1]

[†]**These authors contributed equally to this work.**

1 Research Centre, The Seventh Affiliated Hospital of Sun Yat-sen University, Shenzhen, China

2 Department of Histology and Embryology, Chongqing Key Laboratory of Neurobiology, Brain and Intelligence Research Key Laboratory of Chongqing Education Commission, Third Military Medical University, Chongqing, China

3 School of Life Sciences, University of Technology Sydney, Sydney, NSW 2007, Australia

4 Department of Cell Biology, State Key Laboratory of Trauma, Burn and Combined Injury, Third Military Medical University, Chongqing, China

5 Department of Biochemistry, School of Molecular and Cellular Biology, the University of Illinois at Urbana-Champaign, Urbana, IL 61801, USA

6 Faculty of Biology, Medicine and Health, The University of Manchester, Manchester, UK

7 Achucarro Center for Neuroscience, IKERBASQUE, Basque Foundation for Science, 48011 Bilbao, Spain

Correspondence to: Alexei Verkhratsky
Faculty of Biology, Medicine and Health, The University of Manchester, Manchester, UK
E-mail: Alexej.Verkhratsky@manchester.ac.uk

Correspondence may also be addressed to: Jianqin Niu
Department of Histology and Embryology, Chongqing Key Laboratory of Neurobiology, Brain and Intelligence Research Key Laboratory of Chongqing Education Commission, Third Military

Medical University, Chongqing 400038, China
E-mail: jianqinniu@163.com

Chenju Yi

Research Centre, The Seventh Affiliated Hospital of Sun Yat-sen University, Shenzhen 518107, China

E-mail: yichj@mail.sysu.edu.cn

Running title: Wnt/β-catenin in Alzheimer's disease

Keywords: blood–brain barrier; opsin-free optogenetics; LRP6; Aβ; endothelial cells

Abbreviations: AD = Alzheimer's disease; APP/PS1 = APP_{swe}/$PS1_{dE9}$; BBB = blood–brain barrier; BEC = brain endothelial cells; DKK1 = dickkopf-1; GSK3β = glycogen synthase kinase 3β; LRP6 = LDL Receptor Related Protein 6; PCP = planar cell polarity; PFA = paraformaldehyde; Sox17 = sex determining region Y-box 17; Vangl2 = Vang-like 2 protein; WT = wild-type; Zo-1 = Zonula occludens-1

Abstract

Alzheimer's disease (AD) is a neurodegenerative disorder that causes age-dependent neurological and cognitive declines. The treatments for AD pose a significant challenge, because the mechanisms of disease are not being fully understood. Malfunction of the blood-brain barrier (BBB) is increasingly recognized as a major contributor to the pathophysiology of AD, especially at the early stages of the disease. However, the underlying mechanisms remain poorly characterized, while few molecules can directly target and improve BBB function in the context of AD. Here, we showed dysfunctional BBB in AD patients reflected by perivascular accumulation of blood-derived fibrinogen in the hippocampus and cortex, accompanied by decreased tight junction proteins Claudin-5 and glucose transporter Glut-1 in the brain endothelial cells (BECs). In the $APP_{swe}/PS1_{dE9}$ (APP/PS1) mouse model of AD, BBB dysfunction started at 4 months of age and became severe at 9 months of age. In the cerebral microvessels of APP/PS1 mice and Aβ-treated BECs, we found suppressed Wnt/β-catenin signaling triggered by an increase of GSK3β activation, but not an inhibition of the AKT pathway or switching to the Wnt/planar cell polarity pathway. Furthermore, using our newly developed optogenetic tool for controlled regulation of LRP6 (upstream regulator of the Wnt signaling) to activate Wnt/β-catenin pathway, BBB malfunction was restored by preventing Aβ-induced BEC impairments and promoting the barrier repair. In conclusion, targeting LRP6 in the Wnt/β-catenin pathway in the brain endothelium can alleviate BBB malfunction induced by Aβ, which may be a potential treatment strategy for AD.

Introduction

Alzheimer's disease (AD) is a neurodegenerative disorder that causes age-dependent neurological and cognitive declines. Despite ongoing efforts, the current understanding of AD pathophysiology [1-5] failed to guide to the development of drugs capable of arresting or reversing the disease progression [6,7]. Recent studies have highlighted the dysfunction of the blood-brain barrier (BBB) as an early event of AD [8-12], whereas manipulations with BBB may provide a new target for intervention.

Tight and adherens junction proteins connect adjacent brain endothelial cells (BECs) to seal the BBB, which is composed of endothelial and parenchymal basement membranes, pericytes, and astrocytic endfeet [13,14]. Selective permeability of the BBB restricts the passage of pathogens, and regulates the transport of essential nutrients and metabolites [15]. The impairments of BBB structural components and BECs in particular, compromise the integrity and function of BBB [16]. Pathological changes in BECs are often reflect dysregulation of tight junctions [17], including changes in expression of tight junction protein Claudin-5 [18] and tight junction-actin cytoskeleton connecting protein Zonula occludens-1 (Zo-1) [19]. In a mouse model of AD, reduced expression of glucose transporter Glut-1 in the BECs impaired tight junction integrity and BBB function, leading to cerebral microvascular degeneration [20]. However, the contribution of BBB dysfunction to AD pathogenesis has not been widely acknowledged. A recent study using dynamic contrast-enhanced magnetic resonance imaging (MRI) also found increased BBB permeability in AD brains [8]. This increase in permeability may result in increased levels of albumin, hemoglobin-derived peptides, and prothrombin found in the perivascular brain tissues of AD patients [21-23], although some studies found no significant increase in the extravascular levels of fibrinogen, prealbumin, or immunoglobulins [24,25].

Wnt signaling is critical for the development of BECs [26]. This signaling cascade involves canonical Wnt/β-catenin pathway, non-canonical Wnt/Ca^{2+} pathway, and Wnt/planar cell polarity (PCP) pathway [27]. Tight junction proteins and Glut-1 are the transcriptional targets of Wnt/β-catenin pathway in BECs [26,28,29], while the integrity of endothelial tight junctions is regulated by the Wnt/PCP pathway [30]. The Wnt signaling is significantly reduced in various cell types in the AD brains [31,32]. Which Wnt pathway is specifically involved in the BECs dysfunction in AD pathology remains, however, unknown.

Extracellular amyloid β-protein (Aβ) and its isoforms were shown to regulate Wnt signaling [32-35]. For example, fibrillar Aβ [34] or Aβ oligomer [35] can suppress Wnt/β-catenin pathway in the neurons by binding to the Frizzled receptor of Wnt ligands. In other cell types, Aβ oligomers reduce AKT

activation by increasing the inhibitory regulation of glycogen synthase kinase 3β (GSK3β), with subsequent suppression of the Wnt/β-catenin pathway [36,37]. At the synaptic level, Aβ-induced dickkopf-1 (Dkk1) expression switches from the Wnt/β-catenin pathway to the Wnt/PCP pathway by degrading the Wnt/β-catenin pathway co-receptor LDL Receptor Related Protein 6 (LRP6) [32,38,39]. The Aβ precursor protein (APP) interacts with Vang-like 2 protein (Vangl2) to specifically activate the Wnt/PCP pathway, which drives synapse retraction [32]. Therefore, we aimed to investigate how the Wnt pathway in the BECs is affected at the early stages of AD, and whether this pathway is a plausible target for intervention.

In this study, we firstly demonstrated BBB dysfunction and BEC disruption in postmortem human AD brains. Then in $APP_{swe}/PS1_{dE9}$ (APP/PS1) mouse model of AD, we showed that BBB dysfunction and BEC impairments started at 4 months of age and progressed with aging. In BECs *in vitro,* we found that the Aβ oligomer suppressed the Wnt/β-catenin signaling through the activation of GSK3β, but not through the inhibition of AKT pathway or switching to the Wnt/PCP pathway. Lastly, we provided the evidence that activating Wnt/β-catenin pathway in BECs by targeting its upstream regulator LRP6 can restore Aβ oligomer-induced pathologies, making LRP6 a promising new target for AD drug development.

Materials and methods

Immunohistochemistry for human brain samples

Human post-mortem brain specimens were obtained from the Chinese brain bank center under the ethical approval by the Ethics Committee of the brain bank. The brain specimens were identified as AD by The Brain Bank using the ABC method of AD neuropathologic change, which were categorized into four levels "Not, Low, Intermediate, High" as shown in Supplementary Table 1. After deparaffinization, the paraffin-embedded sections were treated with 3% H_2O_2 and processed for antigen retrieval. The sections were blocked with blocking solution and incubated with targeted primary antibody for 2 h at 37 °C and overnight at 4 °C. After reaction with biotin-specific secondary antibody and signal enhanced by SABC or SABC-AP (Boster) on the following day, the sections were processed with DAB Substrate Kit (Abcam) and BCIP/NBT kit (Boster) for immunoreactive signals detection. The stained sections were dehydrated, mounted in neutral balsam, then examined with a bright field microscope and analyzed by Fuji software. Primary antibodies included: Aβ (1:500, mouse, 800701, BioLegend), CD31 (1:50, rabbit, ab28346, Abcam), Fibrinogen (1:300, mouse, ab58207, Abcam), Cldn5 (1:20, rabbit, 35-2500, Invitrogen), Glut1 (1:100, rabbit, MA5-31960, Invitrogen), Sox17 (1:100, goat, AF1924, R&D). For the quantification, we randomly selected six non-overlapping areas of 1 mm^2 in the cortex and

hippocampus, respectively. Fiji software was used to quantify the fluorescent intensity in each image; then these intensities were averaged for each human brain. Finally, the fluorescent intensities were normalized to the healthy controls. The detailed information of healthy controls and AD patients was listed in Supplementary Table 1.

Animals

C57BL/6J (WT) mice and transgenic APP/PS1 mice were obtained from Nanjing Junke Bioengineering Co., Ltd, China. Male and female Sprague-Dawley rats of 10 days old were obtained from the animal center of Army Medical University, China. All animals used in the study were maintained in a specific-pathogen-free animal facility. All procedures were performed under the ethical approval of the Sun Yat-Sen University Institutional Animal Care and Use Committee.

Immunofluorescence staining

Under deep anesthesia, WT and APP/PS1 mice were perfused intracardially with cold PBS and 4% paraformaldehyde (PFA). The brains were removed, dehydrated, embedded in OCT media and snap-frozen. Cryostat sections (20 μm) were preincubated with blocking buffer (PBS containing 2% BSA and 0.5% Triton-X100) for 30 min. For immunofluorescence staining, BECs on coverslips were fixed with 4% PFA for 15 min and were then permeabilized and blocked with blocking buffer. Sections or coverslips were processed for immunostaining by overnight incubation at 4 °C with primary antibodies, followed by Alexa Fluor conjugated secondary IgG antibodies for 1 h at room temperature. Then, the sections or coverslips were washed, mounted and examined with a confocal microscope. For the quantification of sections, five brain slices from each mouse brain were analyzed. Fiji software was used to quantify the fluorescent intensity, which was averaged for each mouse and then normalized to WT group as relative change. For the quantification of coverslips, three independent experiments with triplicates in each were performed. Five non-overlapping images from each coverslip were analyzed. The values were calculated by fluorescence intensity standardized by DAPI positive cell number in each image by Fiji software, and then normalized to the control group to present the data as relative change and presented as a ratio. Primary antibody for Immunofluorescence included: Aβ (1:200, rabbit, 36-6900, Invitrogen), CD31 (1:200, rat, 553370, BD), Fibrinogen (1:500, mouse, ab58207, Abcam), Cldn5 (1:100, rabbit, 35-2500, Invitrogen), Glut1 (1:200, rabbit, HPA031345, Sigma), CD13 (1:200, rabbit, ab108310, Abcam), IBA1 (1:1000, goat, ab5076, Abcam), GFAP (1:400, rabbit, ab7260, Abcam), Sox17 (1:200, goat, AF1924, R&D), Zo-1 (1:200, mouse, 339100, Invitrogen), Ki67 (1:1000, rabbit, 9129, CST), and Cleaved Caspase-3 (1:400, rabbit, 9661, CST).

Isolation of brain microvessels and primary BECs

The brain microvessels were isolated as previously described [29]. Briefly, the brains were collected and rinsed in ice-cold PBS, and the leptomeninges, cerebellum, brainstem and white matter were removed on ice. The remaining cortices were homogenized in 10 mL of DMEM containing 1 mL 1 mg/mL collagenase (Sigma) and 0.1 mg/mL DNase I (Sigma), and shaken at 250 rpm for 1 h at 37 °C. Then the homogenates were centrifuged at 1000 g for 8 min at room temperature. The pellet was suspended in 25 mL DMEM containing 20% BSA and centrifuged at 1000 g for 20 min at room temperature. The pellet contained the brain microvessels for protein and RNA extraction. For primary BEC culture, the microvessels pellet was further homogenized in 5 mL DMEM containing 0.5 mL 1 mg/mL collagenase-dispase (Roche) and 0.1 mg/mL DNase I, and shaken at 250 rpm for 30 min at 37 °C. The cell pellet was then suspended in BEC culture medium and seeded on collagen-coated plates. Puromycin was supplied in the medium for the first 24 h to achieve high BEC purity.

Protein extraction and Western Blotting

To prepare protein lysates, tissues or cells were lysed in sodium dodecyl sulfate (SDS) lysis buffer supplemented with protease inhibitor cocktail and 2 mM phenylmethylsulfonyl fluoride (PMSF). Protein was quantified by Enhanced BCA Protein Assay Kit (Beyotime), and the normalized protein samples were denatured at 95 °C for 10 min and separated by SDS-polyacrylamide gel electrophoresis. Membranes with transferred proteins were incubated with the primary antibodies overnight at 4 °C followed by secondary antibodies, and detected with the Amersham ECL Prime Western Blotting Detection Reagent (GE Health) by ChampChemi 610 Chemiluminescence Imaging System (Beijing Sage Creation, China). For the quantifications, band densities were measured by Fiji software. The quantification of phosphorylated proteins was normalized to their total proteins. GAPDH was used as the housekeeping protein, and the data were presented as fold change to the control group. Primary antibodies for western blotting included: Cldn5 (1:1000, rabbit, AF5216, Affinity), Glut1 (1:1000, rabbit, ab115730, Abcam), Active β-catenin (1:1000, rabbit, 8814, CST), total β-catenin (1:1000, rabbit, 8480, CST), p-GSK3β (1:1000, mouse, 14630, CST), total GSK3β (1:1000, rabbit, 9315, CST), p-AKT (1:1000, rabbit, 13038, CST), total AKT (1:1000, rabbit, 4691, CST), p-VANGL2 (1:1000, rabbit, MA5-38241, Invitrogen), total VANGL2 (1:1000, rabbit, PA5-23207, Invitrogen), Cleaved Caspase-3 (1:1000, rabbit, 9661, CST), Caspase-3 (1:1000, rabbit, 9662, CST), and GAPDH (1:1000, mouse, AF0006, Beyotime).

RNA-extraction and RT-qPCR

Tissues or cells were washed with ice-cold PBS and then lysed directly by Trizol (Thermo). Total RNA was isolated by RNeasy Plus Mini Kit (Qiagen), and reverse transcription was carried out

using the Reverse Transcriptase kit (Takara), all according to the manufacturer's protocol. qPCR was carried out using FastStart Universal SYBR Green Master Mix (Roche) with Real-time PCR Detection System (Roche). The relative expression of target genes was calculated using the 2 ^-ΔΔ Ct method by normalized to the housekeeping gene GAPDH. The results are presented as a relative change compared to the controls.

Plasmid construction, lentivirus preparation and BEC infection

The plasmid vector was constructed as described previously [40]. The lentivirus was produced using 3rd generation lentiviral generation systems, the virus envelope plasmid, packaging plasmids, and OptoLRP6, ΔCRY2 plasmids were transfected into 293T cell lines. Eight hours after transfection, the media were refreshed. The lentivirus-containing media was collected after 48 h culture and filtered with a 0.22 μm filter. For BEC transfection, lentivirus was added into the culture medium at MOI 20.

Aβ oligomer treatment of the primary BEC

Synthetic $A\beta_{25-35}$ peptide (Sigma) was reconstituted in DMSO (Sigma) and lyophilized overnight. The lyophilized peptide was either processed for oligomer formation or stored at -80 °C for long-term storage. For oligomer formation, the lyophilized stock was resuspended in cell culture medium to the desired concentration and incubated at 37 °C for 24 h to form the oligomers prior to the experiments. The validity of this method has been described previously [41]. Prior to or after light stimulation, BEC was treated with $A\beta_{25-35}$ at 20 μM. All assays were carried out 24 h after exposure to $A\beta_{25-35}$ exposure. At least three independent experiments were performed.

TUNEL assay

Cell apoptosis was detected by TUNEL assay with In Situ Cell Death Detection Kit (Roche) following the manufacturer's protocol. Cells were co-stained with DAPI then subjected to imaging.

Light stimulation

The instrument used for blue-light illumination was described previously [42]. Briefly, the LED box was constructed by plugging blue LED lights into a breadboard containing a 12" x 7" x 3" Aluminum box covered with a translucent plastic board. The LED lights were aligned with the center of each well of the 12-well plate and were wired with resistors. The OptoLRP6-transfected or ΔCRY-transfected cells were illuminated on a 20 min on/40 min off-cycle with blue light. The light intensity was adjusted to 25 LUX at the level of the cells by adjusting the voltage.

In vitro trans-well permeability assay

Primary BECs were seeded on 24-well with a 0.4 μm pore polycarbonate membrane insert trans-

well plate. After receiving desired treatment as described in each group, the cells were subjected to permeability assay. The upper chamber was filled with 150 μL of 1 mg/mL FITC-dextran (40 kDa), while the bottom plate well was replaced with 600 μL fresh BEC culture media. Samples were collected from the bottom well at 30 min. Fluorescence intensities were measured with a microplate reader at 485 nm excitation and 535 nm emission wavelength. The data were compared and normalized to the control group.

Statistical analysis

The differences between two groups were analyzed by a two-tailed Student's *t* test. The differences between multiple groups were analyzed by One-way ANOVA followed by Tukey post hoc tests (GraphPad Prism software). $P < 0.05$ was considered significant, indicated as $* p < 0.05$, $** p < 0.01$. Unless otherwise specified, data were presented as mean ± SEM.

Data availability

The raw data supporting the findings of this study will be made available by the corresponding authors, upon reasonable request.

Results

BBB dysfunction and BEC disruption in AD patients

Dysfunction of the BBB is not universally acknowledged in AD, since there are inconsistencies among studies owing to the sensitivity of the methods [8,21-25,43-45]. In this study, using optimized immunohistochemical double staining method, we investigated five postmortem human AD brains and age- and sex-matched healthy control brains (Supplementary Table 1). Aβ plaques were visible in the hippocampus and cortex of the AD brains (Fig. 1A, B). Fibrinogen, a major blood protein, was detected in the AD brain tissues being accumulated around microvessels (Fig. 1A, B), indicating a vascular leakage. The expression of tight junction protein Claudin-5 was significantly decreased by 40 ± 13.6% in the hippocampus and by 40.5 ± 14.9% in the cortex of AD brains, respectively (both $p < 0.05$, versus control, Fig. 1C). The level of blood vessel co-localized Glut-1 was reduced by 31.8 ± 10.9% in both hippocampus and cortex of AD brains (both $p < 0.05$, versus control, Fig. 1D), suggesting the BBB disruption and BEC dysfunction [46]. These findings are consistent with the pathological changes in BECs in previous studies [10,11,47,48].

BBB dysfunction and BEC disruption occur in the early stage of AD in APP/PS1 mouse model

To assay the timing of BBB dysfunction and BEC malfunction in AD, we used the APP/PS1 mouse

model focusing on the hippocampus. We first examined BBB function in 2, 4 and 9-month-old APP/PS1 mice, representing Aβ amyloidosis at different stages (Supplementary Fig. 1). Aβ deposits started at 4 months of age and were significantly increased at 9 months (Fig. 2A).

Fibrinogen was used as a marker of BBB leakage. In wild-type (WT) controls, fibrinogen can only be detected within the vascular lumen, suggesting intact BBB (Fig. 2B, E). In 4-month-old APP/PS1 mice, a significant extravascular accumulation of fibrinogen was identified in the brain parenchyma (Fig. 2B, E), supporting BBB malfunction in the early stage of AD pathology.

To determine whether BBB malfunction is associated with impaired BECs, we evaluated expression of tight junction protein Claudin-5 and glucose transporter Glut-1 both being essential for maintaining BEC integrity and function [47]. We found that expression of Claudin-5 and Glut-1 were significantly decreased in APP/PS1 mice at 4 and 9 months compared to age-matched WT mice (both markers $p < 0.05$ and $p < 0.01$, respectively, Fig. 2C, D, F, G), consistent with fibrinogen leakage.

Collectively, our results obtained in AD patients and APP/PS1 mouse model indicate that BBB malfunction in AD is linked to BEC impairment. In particular the data obtained in APP/PS1 mice confirm this event occurs at the early stages of AD pathology.

Decreased Wnt/β-catenin signaling in cerebral microvessels of APP/PS1 mice

To identify which Wnt pathway is dysregulated in the BECs in AD, we isolated cerebral microvessels from mouse brains at different ages (Fig. 3A), as evidence suggests that cerebral microvessels can better capture the BBB features thus also enabling mechanistic studies by measuring mRNA and protein changes in tight junction proteins [49]. We found that 99.3 $\pm$ 0.15% of the cells in the isolated cerebral microvessels were identified as CD31-positive BECs (Fig. 3A). Claudin-5 and Glut-1 protein, as well as their mRNA expression, in cerebral microvessels, were significantly decreased at 4 months of age (all $p < 0.05$ versus control) and further reduced at 9 months of age (all $p < 0.01$ versus control) in APP/PS1 mice (Fig. 3B). Similarly, mRNA expression of Zo-1 was also significantly reduced at 4 months of age ($p < 0.05$ versus control), and further reduced at 9 months of age ($p < 0.01$ versus control, Fig. 3C). Occludin mRNA expression was only significantly reduced at 9 months ($p < 0.01$ versus control, Fig. 3C).

The phosphorylation status of the Wnt/β-catenin pathway-related markers, β-catenin and GSK3β, were significantly reduced in cerebral microvessels from APP/PS1 mice at 4 months (β-catenin $p < 0.05$, GSK3β $p < 0.01$ versus control) and 9 months (both β-catenin and GSK3β $p < 0.01$ versus control, Fig. 3D). However, phosphorylated AKT and Vangl2, essential for the PCP pathway activity [45], were not changed in the cerebral microvessels from APP/PS1 mice (Fig. 3E).

Furthermore, reduced Wnt/β-catenin signaling was also confirmed by the down-regulation of its downstream targets, Axin2, Notum and DKK1 mRNA expression in the cerebral microvessels from APP/PS1 mice at 4 and 9 months of age (Fig. 3F).

Taken together, our results demonstrate that the AKT-independent Wnt/β-catenin pathway (as opposed to the Wnt/PCP pathway) was suppressed in cerebral microvessels from APP/PS1 mice.

Aβ oligomer induces impairment of BECs and suppresses the Wnt/β-catenin pathway

We observed BBB and BEC malfunction in 4-month old APP/PS1 mice when soluble Aβ oligomer begins to accumulate to form fibrillar Aβ plaques [50]. As a result, we used primary rat BECs and $A\beta_{25–35}$ fragments (toxic domain of the Aβ) to study Aβ oligomer-related toxicity in BECs [51]. $A\beta_{25–35}$ is the most cytotoxic component of senile plaques and is commonly used to establish the *in vitro* model of BBB malfunction [32-35,52]. Although $A\beta_{1-40}$ was also used to study BBB and cerebrovascular impairments in the literature, the $A\beta_{1-40}$ has low-toxicity and, even showed neuroprotective effects [53-55]; hence we decided not to use it.

We used 20 μM Aβ oligomer ($A\beta_{25–35}$) *in vitro*, because this concentration reduced Claudin-5 without affecting cell proliferation and viability (Supplementary Fig. 2). Exposing BECs to $A\beta_{25–35}$ for 24 hours resulted in a significant decrease in immunoreactivity for Claudin-5 ($p < 0.01$), Zo-1 ($p < 0.05$) and Glut-1 ($p < 0.05$, Fig. 4A). Changes in Claudin-5 ($p < 0.01$) and Glut-1 ($p < 0.05$) were further confirmed by western blotting (Fig. 4B). Reduction in Claudin-5 was also observed at the mRNA level ($p < 0.05$, Fig. 4C). $A\beta_{25–35}$ induced reduction in barrier integrity of BECs was accessed by the permeability assay (Fig. 4D).

Furthermore, 38.8 ± 5.5% reduction in active β-catenin ($p < 0.01$), 41.6 ± 13.3% reduction in phosphorylated Ser9-GSK3β ($p < 0.05$, Fig. 4E), and 29.8 ± 2.5% reduction in Axin2 mRNA expression ($p < 0.01$, Fig. 4F), were observed in $A\beta_{25–35}$-treated BECs *in vitro*. Consistent with the *in vivo* results, AKT and Vangl2 activities in BECs were not affected by $A\beta_{25–35}$ treatment (Fig. 4G), suggesting a specific suppression of the Wnt/β-catenin pathway only in BECs. However, Dkk1 mRNA level was reduced after $A\beta_{25–35}$ treatment ($p < 0.01$, Fig.4H), which may be an adaptive change to the suppressed Wnt/β-catenin signaling.

To further confirm the suppressed Wnt/β-catenin pathway signaling in BECs in AD, the downstream target of Wnt/β-catenin pathway, sex determining region Y-box 17 (Sox17), was quantified. Immunostaining of Sox17 was reduced in the cerebral vessels from both APP/PS1 mice ($p < 0.01$, Fig. 4I) and AD patients ($p < 0.05$, Fig. 4J).

Taken together, our results indicate that $A\beta_{25–35}$ suppressed Wnt/β-catenin activity by reducing BEC markers critical for BBB integrity; the Wnt/β-catenin therefore may be a potential new treatment

target.

Optogenetic activation of Wnt/β-catenin pathway signaling

To achieve a precise regulation of Wnt/β-catenin pathway, we employed an opsin-free optogenetics tool. Opsin-free optogenetics allows light-mediated modulation of the intracellular signaling pathways in live cells with high temporal and spatial accuracy [42,56-59]. Here, we used an in-house developed optogenetic tool (OptoLRP6) [40]. As shown in Fig. 5A, under blue light stimulation, the CRY2-CIBN association allows the interaction between LRP6 and transmembrane protein 198 (TMEM198) to specifically activate LRP6-Wnt signaling [60]. This results in a reversible activation of the Wnt/β-catenin pathway. Based on our preliminary experiments, the light cycling was set to a 20-min-on and 40-min-off mode for maximum light-exposure efficacy and preservation of cell viability.

After light exposure for 8 hours, Axin2 mRNA expression ($p<0.01$, Fig. 5B), active β-catenin ($p<0.05$, Fig. 5C), and phosphorylated Ser9-GSK3β ($p<0.01$, Fig. 5C) were all increased in light-stimulated OptoLRP6-infected BECs compared with control ΔCRY plasmid-transfected BECs. However, AKT and Vangl2 activities, as well as Dkk1 mRNA level, remained unchanged, confirming that targeting OptoLRP6 exclusively activates the Wnt/β-catenin pathway, but not the Wnt/PCP pathway.

Light-induced OptoLRP6 activation rescued $A\beta_{25–35}$-induced BEC impairment

We then treated OptoLRP6 or control ΔCRY plasmid-transfected BECs with $A\beta_{25–35}$ for 24 hours, followed by light exposure for 8 hours (Fig. 6A). After light stimulation, Axin2 level in the $A\beta_{25–35}$ treated OptoLRP6-transfected group was the highest ($p < 0.01$ versus all other 3 groups, Fig. 6B). The suppressed immunoreactivities of Claudin-5, Zo-1, and Glut-1 were significantly recovered by light stimulation in the OptoLRP6 group after the exposure to $A\beta_{25–35}$ (Fig. 6C), consistent with the results of Wnt ligand Wnt3a treatment (Supplementary Fig. 3). Changes in Claudin-5 were confirmed by both western blotting (Fig. 6D) and qPCR (Fig. 6E), while changes in Glut-1 were confirmed by western blotting (Fig. 6D). The dye-tracers experiment confirmed the improvement of BBB permeability in BECs transfected with OptoLRP6 and illuminated (Fig. 6F). The results suggest that the activation of the Wnt/β-catenin pathway by targeting LRP6 has the potential therapeutic value to rescue Aβ-induced BBB malfunction in AD.

Pre-activation of the Wnt/β-catenin pathway by OptoLRP6 prevents $A\beta_{25–35}$-induced BEC disruption

BECs impairment at an early stage of AD pathology in APP/PS1 mice suggests that BBB malfunction may contribute to AD pathogenesis. Therefore, we investigated whether pre-activation

of the Wnt/β-catenin pathway can prevent Aβ-induced BEC impairments. Primary BECs transfected with OptoLRP6 or control ΔCRY plasmid were stimulated by blue light for 8 hours, followed by exposure to $A\beta_{25–35}$ for 24 hours (Fig. 7A).

Axin2 levels were significantly increased in BECs transfected with OptoLRP6 after light and $A\beta_{25–35}$ exposure as compared to all the other ΔCRY groups (all $p < 0.01$, Fig. 7B). The protein levels of tight junction proteins Claudin-5, Zo-1, and glucose transporter Glut-1 in BECs transfected with OptoLRP6 were nearly the same as controls (Fig. 7C-E), in line with the results of Wnt ligand Wnt3a treatment (Supplementary Fig. 3). The dye-tracers experiment also confirmed the improvement of BBB permeability *in vitro* (Fig. 7F). These data suggest the preventive effects of activated Wnt/β-catenin signaling against $A\beta_{25–35}$-induced BEC dysfunction.

Discussion

This study confirmed that BBB malfunction caused by impaired BECs plays a key role in the early stage of AD pathophysiology [8-12,61,62]. By using both human AD specimens and APP/PS1 mice, we found that BBB damage stemmed from reduced levels of tight junction proteins and glucose transporter Glut-1. Dysregulation of Wnt/β-catenin pathway signaling in cerebral microvessels by Aβ oligomer may be the underlying mechanism of BEC impairment in AD. Using a novel optogenetic tool, we discovered a promising new target for treatment strategies, the Wnt co-receptor LRP6, which can effectively activate Wnt/β-catenin pathway to protect BECs against $A\beta_{25–35}$-induced toxicity and restore BEC abnormalities in AD (Fig. 8).

It is widely acknowledged that BBB malfunction contributes to many neuropathologies [47,63,64], although there are still inconsistencies in showing the extravasation of plasma-derived proteins [8,21-25,43-45]. Nonetheless, leakage of blood protein fibrinogen into perivascular tissue following the breakdown of BBB is increasingly recognized as a contributor to neuropathology [65]. Deploying neuroprotectant to rescue behavioral deficits in AD model simultaneously improved BBB and cerebrovascular integrity, along with reduced Aβ formation [66]. However, it is difficult to determine whether the vascular protection was primary or secondary to reduced Aβ accumulation. In the present study, we showed that BBB integrity is impaired in AD patients and APP/PS1 mice, as indicated by increased levels of plasma-derived fibrinogen in extravascular tissues and decreased levels of BEC tight junction proteins and Glut-1. In particular, our data in APP/PS1 mice confirm that this sign occurs at the early stages of AD. This suggests that fibrinogen may be used as a new imaging biomarker of dysfunctional BECs and BBB in humans, and/or early diagnosis of AD. However, as the information on familial or sporadic AD was not registered at the Brain Bank, it remains unclear which specific AD type was investigated.

BEC-related pathologies occur in the early stages of AD. Thus, it is natural to ask the question of whether targeting repair of BECs can protect BBB function and thereafter prevent/reverse the decline of the AD brain. To better understand the mechanisms that impair BECs in AD, Wnt pathway was studied because of its involvement in BEC pathologies [26,28,29] and association with risk factors of AD, such as LRP6, GSK3β, Dkk1 and Vangl2 [67,68]. In the brains of both AD patients and APP/PS1 mice, we discovered a significant reduction in Wnt/β-catenin pathway activity, mostly driven by the suppressed upstream regulator LRP6. Other regulators, such as GSK3β and AKT, as well as Wnt/PCP pathway, did not seem to be involved. Moreover, we demonstrate that $A\beta_{25-35}$ induced BBB dysfunction and BEC disruption through suppressing the canonical Wnt/β-catenin pathway signaling [26]. This effect may be mediated by $A\beta_{25-35}$ binding to Frizzled receptors, which are required to activate the Wnt/β-catenin pathway by LRP6 [35], while we can exclude AKT signaling and the non-canonical Wnt/PCP pathway. In addition, we found a significant decrease in Dkk1 in BECs in APP/PS1 mice, contrary to previously reported increases in Dkk1 in neurons [32,69], with the underlying mechanism still unknown. Nevertheless, our findings provide a plausible mechanism of the pathogenesis of BBB and BEC dysfunction in AD brains, which may exacerbate AD neuropathology [70,71]. Protecting or reversing vascular function may slow down the decline or preserve neurological function.

In order to determine whether Wnt/β-catenin pathway, particularly its upstream regulator LRP6, is a valid target to protect cerebrovascular function, we adopted a novel optogenetic technique to accurately regulate LRP6 on the cell surface to activate Wnt/β-catenin pathway signaling, since the Wnt ligand is unable to target the canonical Wnt/β-catenin pathway exclusively [72]. LRP6 has been linked to synaptic and cognitive abnormalities in aged mice and AD patients [31,73]. Curcumin, a natural compound, has been demonstrated to increase LRP6 levels to exert potential neuroprotective effects in several AD animal models [74-76]; however, it is not suitable for AD treatment due to its low bioavailability. In this study, using our optogenetic tool, we showed that increasing the Wnt/β-catenin signaling by activating LRP6 partially restored expression of tight junction proteins Claudin-5, Zo-1 and glucose transporter Glut-1 after $A\beta_{25-35}$ exposure, suggesting such approach may be used as a potential therapeutic strategy to alleviate or even reverse $A\beta_{25-35}$-induced BBB malfunction in AD patients. Furthermore, activation of Wnt/β-catenin pathway signaling can also prevent pathological changes in BECs induced by $A\beta_{25-35}$ exposure, suggesting the potential for LRP6 as a preventive treatment to protect BBB function in AD. However, whether targeting LRP6 can also reduce/clear Aβ accumulation and preserve neurological function needs to be examined in future in APP/PS1 mice at different ages.

In conclusion, BBB dysfunction due to BECs disruption is present in human AD brains, and occurs

at the early stages of AD pathogenesis in APP/PS1 mice. In BECs, targeting the Wnt/β-catenin pathway upstream co-receptor LRP6 can restore the Aβ oligomer-induced pathologies, suggesting LRP6 as a new potential target for AD treatment.

Funding

This study was supported by grants from the National Natural Science Foundation of China (NSFC 81971309, 32170980, 32070964, 31871045), National Key Research and Development Program of China (2017YFA0106000, 2021ZD0201703), Guangdong Basic and Applied Basic Research Foundation (2022B1515020012, 2019A1515011333), and Shenzhen Basic Research Foundation (RCYX20200714114644167, JCYJ20210324123212035, JCYJ20190809161405495).

Competing interests

The authors declare no competing interests.

Supplementary material

Supplementary material is available at *Brain* online.

References

1. Kraepelin E. *Psychiatrie; ein Lehrbuch für Studierende und Ärzte*. vol 2. Barth; 1910.
2. De Strooper B, Karran E. The Cellular Phase of Alzheimer's Disease. *Cell*. Feb 11 2016;164(4):603-15. doi:10.1016/j.cell.2015.12.056
3. Liu PP, Xie Y, Meng XY, Kang JS. History and progress of hypotheses and clinical trials for Alzheimer's disease. *Signal Transduct Target Ther*. 2019;4:29. doi:10.1038/s41392-019-0063-8
4. Long JM, Holtzman DM. Alzheimer Disease: An Update on Pathobiology and Treatment Strategies. *Cell*. Oct 3 2019;179(2):312-339. doi:10.1016/j.cell.2019.09.001
5. Guo T, Zhang D, Zeng Y, Huang TY, Xu H, Zhao Y. Molecular and cellular mechanisms underlying the pathogenesis of Alzheimer's disease. *Mol Neurodegener*. Jul 16 2020;15(1):40. doi:10.1186/s13024-020-00391-7
6. Huang J, Shen M, Qin X, Wu M, Liang S, Huang Y. Acupuncture for the Treatment of Alzheimer's Disease: An Overview of Systematic Reviews. *Front Aging Neurosci*. 2020;12:574023. doi:10.3389/fnagi.2020.574023
7. Tolar M, Abushakra S, Sabbagh M. The path forward in Alzheimer's disease therapeutics: Reevaluating the amyloid cascade hypothesis. *Alzheimers Dement*. Nov 2020;16(11):1553-1560. doi:10.1016/j.jalz.2019.09.075
8. Montagne A, Barnes SR, Sweeney MD, et al. Blood-brain barrier breakdown in the aging human hippocampus. *Neuron*. Jan 21 2015;85(2):296-302. doi:10.1016/j.neuron.2014.12.032
9. Yamazaki Y, Kanekiyo T. Blood-Brain Barrier Dysfunction and the Pathogenesis of Alzheimer's Disease. *Int J Mol Sci*. Sep 13 2017;18(9)doi:10.3390/ijms18091965
10. van de Haar HJ, Burgmans S, Jansen JF, et al. Blood-Brain Barrier Leakage in Patients with Early Alzheimer Disease. *Radiology*. Nov 2016;281(2):527-535. doi:10.1148/radiol.2016152244
11. Nation DA, Sweeney MD, Montagne A, et al. Blood-brain barrier breakdown is an early biomarker of human cognitive dysfunction. *Nat Med*. Feb 2019;25(2):270-276. doi:10.1038/s41591-018-0297-y
12. Montagne A, Nation DA, Sagare AP, et al. APOE4 leads to blood-brain barrier dysfunction predicting cognitive decline. *Nature*. May 2020;581(7806):71-76. doi:10.1038/s41586-020-2247-3
13. Langen UH, Ayloo S, Gu C. Development and Cell Biology of the Blood-Brain Barrier. *Annu Rev Cell Dev Biol*. Oct 6 2019;35:591-613. doi:10.1146/annurev-cellbio-100617-062608
14. Huang Z, Wong LW, Su Y, et al. Blood-brain barrier integrity in the pathogenesis of Alzheimer's disease. *Front Neuroendocrinol*. Aug 8 2020;59:100857. doi:10.1016/j.yfrne.2020.100857
15. Profaci CP, Munji RN, Pulido RS, Daneman R. The blood-brain barrier in health and disease: Important unanswered questions. *J Exp Med*. Apr 6 2020;217(4)doi:10.1084/jem.20190062
16. Kadry H, Noorani B, Cucullo L. A blood-brain barrier overview on structure, function, impairment, and biomarkers of integrity. *Fluids Barriers CNS*. Nov 18 2020;17(1):69. doi:10.1186/s12987-020-00230-3
17. Bauer HC, Krizbai IA, Bauer H, Traweger A. "You Shall Not Pass"-tight junctions of the blood brain barrier. *Front Neurosci*. 2014;8:392. doi:10.3389/fnins.2014.00392
18. Morita K, Sasaki H, Furuse M, Tsukita S. Endothelial claudin: claudin-5/TMVCF constitutes tight junction strands in endothelial cells. *J Cell Biol*. Oct 4 1999;147(1):185-94. doi:10.1083/jcb.147.1.185
19. Tornavaca O, Chia M, Dufton N, et al. ZO-1 controls endothelial adherens junctions, cell-

cell tension, angiogenesis, and barrier formation. *J Cell Biol*. Mar 16 2015;208(6):821-38. doi:10.1083/jcb.201404140
20. Winkler EA, Nishida Y, Sagare AP, et al. GLUT1 reductions exacerbate Alzheimer's disease vasculo-neuronal dysfunction and degeneration. *Nat Neurosci*. Apr 2015;18(4):521-530. doi:10.1038/nn.3966
21. Wisniewski HM, Kozlowski PB. Evidence for blood-brain barrier changes in senile dementia of the Alzheimer type (SDAT). *Ann N Y Acad Sci*. 1982;396:119-29. doi:10.1111/j.1749-6632.1982.tb26848.x
22. Slemmon JR, Hughes CM, Campbell GA, Flood DG. Increased levels of hemoglobin-derived and other peptides in Alzheimer's disease cerebellum. *J Neurosci*. Apr 1994;14(4):2225-35.
23. Zipser BD, Johanson CE, Gonzalez L, et al. Microvascular injury and blood-brain barrier leakage in Alzheimer's disease. *Neurobiol Aging*. Jul 2007;28(7):977-86. doi:10.1016/j.neurobiolaging.2006.05.016
24. Alafuzoff I, Adolfsson R, Grundke-Iqbal I, Winblad B. Blood-brain barrier in Alzheimer dementia and in non-demented elderly. An immunocytochemical study. *Acta Neuropathol*. 1987;73(2):160-6. doi:10.1007/BF00693782
25. Tomimoto H, Akiguchi I, Suenaga T, et al. Alterations of the blood-brain barrier and glial cells in white-matter lesions in cerebrovascular and Alzheimer's disease patients. *Stroke*. Nov 1996;27(11):2069-74. doi:10.1161/01.str.27.11.2069
26. Liebner S, Corada M, Bangsow T, et al. Wnt/beta-catenin signaling controls development of the blood-brain barrier. *J Cell Biol*. Nov 3 2008;183(3):409-17. doi:10.1083/jcb.200806024
27. Komiya Y, Habas R. Wnt signal transduction pathways. *Organogenesis*. Apr 2008;4(2):68-75. doi:10.4161/org.4.2.5851
28. Laksitorini MD, Yathindranath V, Xiong W, Hombach-Klonisch S, Miller DW. Modulation of Wnt/beta-catenin signaling promotes blood-brain barrier phenotype in cultured brain endothelial cells. *Sci Rep*. Dec 23 2019;9(1):19718. doi:10.1038/s41598-019-56075-w
29. Niu J, Tsai HH, Hoi KK, et al. Aberrant oligodendroglial-vascular interactions disrupt the blood-brain barrier, triggering CNS inflammation. *Nat Neurosci*. May 2019;22(5):709-718. doi:10.1038/s41593-019-0369-4
30. Artus C, Glacial F, Ganeshamoorthy K, et al. The Wnt/planar cell polarity signaling pathway contributes to the integrity of tight junctions in brain endothelial cells. *J Cereb Blood Flow Metab*. Mar 2014;34(3):433-40. doi:10.1038/jcbfm.2013.213
31. Liu CC, Tsai CW, Deak F, et al. Deficiency in LRP6-mediated Wnt signaling contributes to synaptic abnormalities and amyloid pathology in Alzheimer's disease. *Neuron*. Oct 1 2014;84(1):63-77. doi:10.1016/j.neuron.2014.08.048
32. Elliott C, Rojo AI, Ribe E, et al. A role for APP in Wnt signalling links synapse loss with beta-amyloid production. *Transl Psychiatry*. Sep 20 2018;8(1):179. doi:10.1038/s41398-018-0231-6
33. De Ferrari GV, Inestrosa NC. Wnt signaling function in Alzheimer's disease. *Brain Res Brain Res Rev*. Aug 2000;33(1):1-12. doi:10.1016/s0165-0173(00)00021-7
34. Garrido JL, Godoy JA, Alvarez A, Bronfman M, Inestrosa NC. Protein kinase C inhibits amyloid beta peptide neurotoxicity by acting on members of the Wnt pathway. *FASEB J*. Dec 2002;16(14):1982-4. doi:10.1096/fj.02-0327fje
35. Magdesian MH, Carvalho MM, Mendes FA, et al. Amyloid-beta binds to the extracellular cysteine-rich domain of Frizzled and inhibits Wnt/beta-catenin signaling. *J Biol Chem*. Apr 4 2008;283(14):9359-68. doi:10.1074/jbc.M707108200

36. Park KS, Lee RD, Kang SK, et al. Neuronal differentiation of embryonic midbrain cells by upregulation of peroxisome proliferator-activated receptor-gamma via the JNK-dependent pathway. *Exp Cell Res*. Jul 15 2004;297(2):424-33. doi:10.1016/j.yexcr.2004.03.034
37. Yue X, Lan F, Yang W, et al. Interruption of beta-catenin suppresses the EGFR pathway by blocking multiple oncogenic targets in human glioma cells. *Brain Res*. Dec 17 2010;1366:27-37. doi:10.1016/j.brainres.2010.10.032
38. Sellers KJ, Elliott C, Jackson J, et al. Amyloid beta synaptotoxicity is Wnt-PCP dependent and blocked by fasudil. *Alzheimers Dement*. Mar 2018;14(3):306-317. doi:10.1016/j.jalz.2017.09.008
39. Mao B, Wu W, Li Y, et al. LDL-receptor-related protein 6 is a receptor for Dickkopf proteins. *Nature*. May 17 2001;411(6835):321-5. doi:10.1038/35077108
40. Krishnamurthy VV, Hwang H, Fu J, Yang J, Zhang K. Optogenetic Control of the Canonical Wnt Signaling Pathway During Xenopus laevis Embryonic Development. *J Mol Biol*. May 19 2021:167050. doi:10.1016/j.jmb.2021.167050
41. Millucci L, Raggiaschi R, Franceschini D, Terstappen G, Santucci A. Rapid aggregation and assembly in aqueous solution of A beta (25-35) peptide. *J Biosci*. Jun 2009;34(2):293-303. doi:10.1007/s12038-009-0033-3
42. Su Y, Huang X, Huang Z, et al. Early But Not Delayed Optogenetic RAF Activation Promotes Astrocytogenesis in Mouse Neural Progenitors. *J Mol Biol*. Jul 24 2020;432(16):4358-4368. doi:10.1016/j.jmb.2020.06.020
43. Schlageter NL, Carson RE, Rapoport SI. Examination of blood-brain barrier permeability in dementia of the Alzheimer type with [68Ga]EDTA and positron emission tomography. *J Cereb Blood Flow Metab*. Feb 1987;7(1):1-8. doi:10.1038/jcbfm.1987.1
44. Dysken MW, Nelson MJ, Hoover KM, Kuskowski M, McGeachie R. Rapid dynamic CT scanning in primary degenerative dementia and age-matched controls. *Biol Psychiatry*. Sep 1 1990;28(5):425-34. doi:10.1016/0006-3223(90)90410-4
45. Caserta MT, Caccioppo D, Lapin GD, Ragin A, Groothuis DR. Blood-brain barrier integrity in Alzheimer's disease patients and elderly control subjects. *J Neuropsychiatry Clin Neurosci*. Winter 1998;10(1):78-84. doi:10.1176/jnp.10.1.78
46. Obermeier B, Daneman R, Ransohoff RM. Development, maintenance and disruption of the blood-brain barrier. *Nat Med*. Dec 2013;19(12):1584-96. doi:10.1038/nm.3407
47. Zlokovic BV. The blood-brain barrier in health and chronic neurodegenerative disorders. *Neuron*. Jan 24 2008;57(2):178-201. doi:10.1016/j.neuron.2008.01.003
48. Montagne A, Zhao Z, Zlokovic BV. Alzheimer's disease: A matter of blood-brain barrier dysfunction? *J Exp Med*. Nov 6 2017;214(11):3151-3169. doi:10.1084/jem.20171406
49. Navone SE, Marfia G, Invernici G, et al. Isolation and expansion of human and mouse brain microvascular endothelial cells. *Nat Protoc*. Sep 2013;8(9):1680-93. doi:10.1038/nprot.2013.107
50. Larson ME, Lesne SE. Soluble Abeta oligomer production and toxicity. *J Neurochem*. Jan 2012;120 Suppl 1:125-139. doi:10.1111/j.1471-4159.2011.07478.x
51. Millucci L, Ghezzi L, Bernardini G, Santucci A. Conformations and biological activities of amyloid beta peptide 25-35. *Curr Protein Pept Sci*. Feb 2010;11(1):54-67. doi:10.2174/138920310790274626
52. Cuevas E, Rosas-Hernandez H, Burks SM, et al. Amyloid Beta 25-35 induces blood-brain barrier disruption in vitro. *Metab Brain Dis*. Oct 2019;34(5):1365-1374. doi:10.1007/s11011-019-00447-8
53. Zou K, Kim D, Kakio A, et al. Amyloid beta-protein (Abeta)1-40 protects neurons from

damage induced by Abeta1-42 in culture and in rat brain. *J Neurochem*. Nov 2003;87(3):609-19. doi:10.1046/j.1471-4159.2003.02018.x
54. Merino-Zamorano C, Fernandez-de Retana S, Montanola A, et al. Modulation of Amyloid-beta1-40 Transport by ApoA1 and ApoJ Across an in vitro Model of the Blood-Brain Barrier. *J Alzheimers Dis*. May 25 2016;53(2):677-91. doi:10.3233/JAD-150976
55. Wang D, Chen F, Han Z, Yin Z, Ge X, Lei P. Relationship Between Amyloid-beta Deposition and Blood-Brain Barrier Dysfunction in Alzheimer's Disease. *Front Cell Neurosci*. 2021;15:695479. doi:10.3389/fncel.2021.695479
56. Tischer D, Weiner OD. Illuminating cell signalling with optogenetic tools. *Nat Rev Mol Cell Biol*. Aug 2014;15(8):551-8. doi:10.1038/nrm3837
57. Zhang K, Cui B. Optogenetic control of intracellular signaling pathways. *Trends Biotechnol*. Feb 2015;33(2):92-100. doi:10.1016/j.tibtech.2014.11.007
58. Huang T, Zhang Y, Wang Z, et al. Optogenetically Controlled TrkA Activity Improves the Regenerative Capacity of Hair-Follicle-Derived Stem Cells to Differentiate into Neurons and Glia. *Adv Biosyst*. Sep 13 2020:e2000134. doi:10.1002/adbi.202000134
59. Shin G, Gomez AM, Al-Hasani R, et al. Flexible Near-Field Wireless Optoelectronics as Subdermal Implants for Broad Applications in Optogenetics. *Neuron*. Feb 8 2017;93(3):509-521 e3. doi:10.1016/j.neuron.2016.12.031
60. Liang J, Fu Y, Cruciat CM, et al. Transmembrane protein 198 promotes LRP6 phosphorylation and Wnt signaling activation. *Mol Cell Biol*. Jul 2011;31(13):2577-90. doi:10.1128/MCB.05103-11
61. Kalaria RN, Hedera P. Differential degeneration of the cerebral microvasculature in Alzheimer's disease. *Neuroreport*. Feb 15 1995;6(3):477-80. doi:10.1097/00001756-199502000-00018
62. Zenaro E, Piacentino G, Constantin G. The blood-brain barrier in Alzheimer's disease. *Neurobiol Dis*. Nov 2017;107:41-56. doi:10.1016/j.nbd.2016.07.007
63. Erickson MA, Banks WA. Blood-brain barrier dysfunction as a cause and consequence of Alzheimer's disease. *J Cereb Blood Flow Metab*. Oct 2013;33(10):1500-13. doi:10.1038/jcbfm.2013.135
64. Sweeney MD, Zhao Z, Montagne A, Nelson AR, Zlokovic BV. Blood-Brain Barrier: From Physiology to Disease and Back. *Physiol Rev*. Jan 1 2019;99(1):21-78. doi:10.1152/physrev.00050.2017
65. Petersen MA, Ryu JK, Akassoglou K. Fibrinogen in neurological diseases: mechanisms, imaging and therapeutics. *Nat Rev Neurosci*. May 2018;19(5):283-301. doi:10.1038/nrn.2018.13
66. Lazic D, Sagare AP, Nikolakopoulou AM, Griffin JH, Vassar R, Zlokovic BV. 3K3A-activated protein C blocks amyloidogenic BACE1 pathway and improves functional outcome in mice. *J Exp Med*. Feb 4 2019;216(2):279-293. doi:10.1084/jem.20181035
67. Kibar Z, Vogan KJ, Groulx N, Justice MJ, Underhill DA, Gros P. Ltap, a mammalian homolog of Drosophila Strabismus/Van Gogh, is altered in the mouse neural tube mutant Loop-tail. *Nat Genet*. Jul 2001;28(3):251-5. doi:10.1038/90081
68. Rao TP, Kuhl M. An updated overview on Wnt signaling pathways: a prelude for more. *Circ Res*. Jun 25 2010;106(12):1798-806. doi:10.1161/CIRCRESAHA.110.219840
69. Killick R, Ribe EM, Al-Shawi R, et al. Clusterin regulates beta-amyloid toxicity via Dickkopf-1-driven induction of the wnt-PCP-JNK pathway. *Mol Psychiatry*. Jan 2014;19(1):88-98. doi:10.1038/mp.2012.163
70. Bhat RV, Andersson U, Andersson S, Knerr L, Bauer U, Sundgren-Andersson AK. The

Conundrum of GSK3 Inhibitors: Is it the Dawn of a New Beginning? *J Alzheimers Dis*. 2018;64(s1):S547-S554. doi:10.3233/JAD-179934
71. Athar T, Al Balushi K, Khan SA. Recent advances on drug development and emerging therapeutic agents for Alzheimer's disease. *Mol Biol Rep*. Jul 2021;48(7):5629-5645. doi:10.1007/s11033-021-06512-9
72. Samarzija I, Sini P, Schlange T, Macdonald G, Hynes NE. Wnt3a regulates proliferation and migration of HUVEC via canonical and non-canonical Wnt signaling pathways. *Biochem Biophys Res Commun*. Aug 28 2009;386(3):449-54. doi:10.1016/j.bbrc.2009.06.033
73. Alarcon MA, Medina MA, Hu Q, et al. A novel functional low-density lipoprotein receptor-related protein 6 gene alternative splice variant is associated with Alzheimer's disease. *Neurobiol Aging*. Jun 2013;34(6):1709 e9-18. doi:10.1016/j.neurobiolaging.2012.11.004
74. Tiwari SK, Agarwal S, Seth B, et al. Curcumin-loaded nanoparticles potently induce adult neurogenesis and reverse cognitive deficits in Alzheimer's disease model via canonical Wnt/beta-catenin pathway. *ACS Nano*. Jan 28 2014;8(1):76-103. doi:10.1021/nn405077y
75. Farkhondeh T, Samarghandian S, Pourbagher-Shahri AM, Sedaghat M. The impact of curcumin and its modified formulations on Alzheimer's disease. *J Cell Physiol*. Aug 2019;234(10):16953-16965. doi:10.1002/jcp.28411
76. Sanei M, Saberi-Demneh A. Effect of curcumin on memory impairment: A systematic review. *Phytomedicine*. Jan 2019;52:98-106. doi:10.1016/j.phymed.2018.06.016

Figure legends

Figure 1 BBB dysfunction and BEC disruption in postmortem AD brains. (A) Fibrinogen/CD31, Cldn5 and Aβ/Glut1 staining in the cortex and **(B)** hippocampus of postmortem health control and patients with AD. **(C)** Quantification of Cldn5 and **(D)** Glut1 intensity and **(E)** Aβ plaques in the cortex and hippocampus of healthy controls and AD patients. Black frames in the low-magnification images indicate the location of the high-magnification images at the right. Arrows indicate Aβ plaques, and arrowheads indicate the fibrinogen leakage and decreased Cldn5 and Glut1 in AD patients. Scale bar: 200 μm in (A) and (B). Data are presented as mean ± SEM, *n = 5, * p < 0.05, ** p < 0.01.*

Figure 2 BBB dysfunction and BEC disruption presented at an early stage of AD pathogenesis in APP/PS1 mice. (A) Immunostaining of Aβ in the hippocampus of 2, 4 and 9-month old wide-type (WT) and $APP_{swe}/PS1_{dE9}$ (APP/PS1) mice (Scale bar: 500 μm). **(B)** Immunostaining of Fibrinogen and CD31 in the hippocampus of 2, 4 and 9-month old WT and APP/PS1 mice (Scale bar: 20 μm). **(C)** Immunostaining of Cldn5 in the hippocampus of 4-month and 9-month WT and APP/PS1 mice (Scale bar: 20 μm). **(D)** Immunostaining of Glut1 in the hippocampus of 4-month and 9-month old WT and APP/PS1 mice (Scale bar: 20 μm). Arrowheads indicate the markers of interest in APP/PS1 mice. **(E-G)** Quantification of Fibrinogen, Cldn5 and Glut1 in the hippocampus of 2, 4 and 9-month old WT and APP/PS1 mice. Data are presented as mean ± SEM, *n = 5, * p < 0.05, ** p < 0.01.*

Figure 3 Decreased Wnt/β-catenin pathway in cerebral microvessels of APP/PS1 mice. (A) Schematic diagram of cerebral microvessels isolation. Representative immunostaining images of markers for (**i** and **ii**) endothelium (CD31), astrocyte (GFAP), (**iii**) microglia (IBA1), and (**iv**) pericyte (CD13) (Scale bar: 100 μm). **(B)** Protein levels of Cldn5 and Glut1 in isolated cerebral microvessels of 2, 4 and 9-month old WT and APP/PS1 mice. **(C)** mRNA expression of Cldn5, Zo1, Glut1, Ocldn and CD31 in microvessels from 2, 4 and 9-month old WT and APP/PS1 mice. **(D)** Protein levels of active β-catenin and phosphorylated Ser9-GSK3β in microvessels form 2, 4 and 9-month old WT and APP/PS1 mice. **(E)** Protein levels of AKT and Vangl2 in microvessels of 2, 4 and 9-month old WT and APP/PS1 mice. **(F)** mRNA expression of canonical Wnt pathway targets Axin2, Notum and DKK1 in microvessels of 2, 4 and 9-month old WT and APP/PS1 mice. Data are presented mean ± SEM, *n = 6* in 2 and 9-month group, *n = 8* in 4-month group for western blot experiment; *n = 5* for RT-qPCR experiment; * *p < 0.05, ** p < 0.01*.

Figure 4 Aβ oligomer treatment induces BEC disruption and downregulates Wnt/β-catenin signaling elements. (A) Immunostaining and quantification of Cldn5, Zo1 and Glut1 in control and Aβ treated BECs (Scale bar: 20 μm). **(B)** Protein levels of Cldn5 and Glut1, **(C)** mRNA expression of Cldn5, **(D)** In vitro trans-well permeability assay, **(E)** protein levels of active β-catenin and phosphorylated Ser9-GSK3β, **(F)** mRNA expression of Axin2, **(G)** protein levels of AKT and Vangl2 and **(H)** mRNA expression of DKK1 in control and Aβ treated BECs. **(I)** Immunostaining and quantification of Sox17 in 4-month old WT and APP/PS1 mice (Scale bar: 50 μm). **(J)** Sox17 levels in the cortex of health control and AD patients (Scale bar: 50 μm). Data are presented as mean ± SEM, $n = 3$ in (B-H), $n = 5$ in (A, I, J), * $p < 0.05$, ** $p < 0.01$.

Figure 5 Optogenetic activation of Wnt/β-catenin pathway. (A) Schematic diagram of the optogenetic method. **(B)** Axin2 mRNA expression, **(C)** protein levels of active β-catenin and phosphorylated Ser9-GSK3β, **(D)** protein level of AKT and Vangl2, **(E)** DKK1 mRNA expression in the BECs. Data are presented as mean ± SEM, n = 3, * $p < 0.05$, ** $p < 0.01$.

Figure 6 Light stimulated OptoLRP6 activation rescues BEC disruption after Aβ oligomer treatment. (A) Schematic diagram of experiment design. **(B)** Axin2 mRNA expression, **(C)** immunostaining and quantification of Cldn5, Zo1 and Glut1 (Scale bar: 20 μm), **(D)** protein levels of Cldn5 and Glut1, **(E)** Cldn5 mRNA expression, **(F)** In vitro trans-well permeability assay in BECs. Data are presented as mean ± SEM, $n = 3$, * $p < 0.05$, ** $p < 0.01$.

Figure 7 Activation of the Wnt/β-catenin pathway by OptoLRP6 prevents Aβ oligomer-induced BEC disruption. (A) Schematic diagram of experiment design. **(B)** Axin2 mRNA expression, **(C)** immunostaining and quantification of Cldn5, Zo1 and Glut1 (Scale bar: 20 μm), **(D)** protein levels of Cldn5 and Glut1, **(E)** Cldn5 mRNA expression, **(F)** In vitro trans-well permeability assay in BECs. Data are presented as mean ± SEM, $n = 3$, * $p < 0.05$, ** $p < 0.01$.

Figure 8 Targeting LRP6 in the Wnt/β-catenin pathway in brain endothelial cells alleviates blood-brain barrier dysfunction. In the Alzheimer's disease (AD) brain, Aβ oligomers suppress Wnt/β-catenin signaling in the brain endothelial cells (BECs), leading to reduced expression of endothelial functional proteins and blood brain barrier (BBB) malfunction. Our recently developed optogenetic tool allows precise regulation of LRP6, the upstream regulator of Wnt/β-catenin signaling. The activation of Wnt/β-catenin signaling restored Aβ-inhibited BEC function by reversing and preventing Aβ-induced BEC pathological changes.

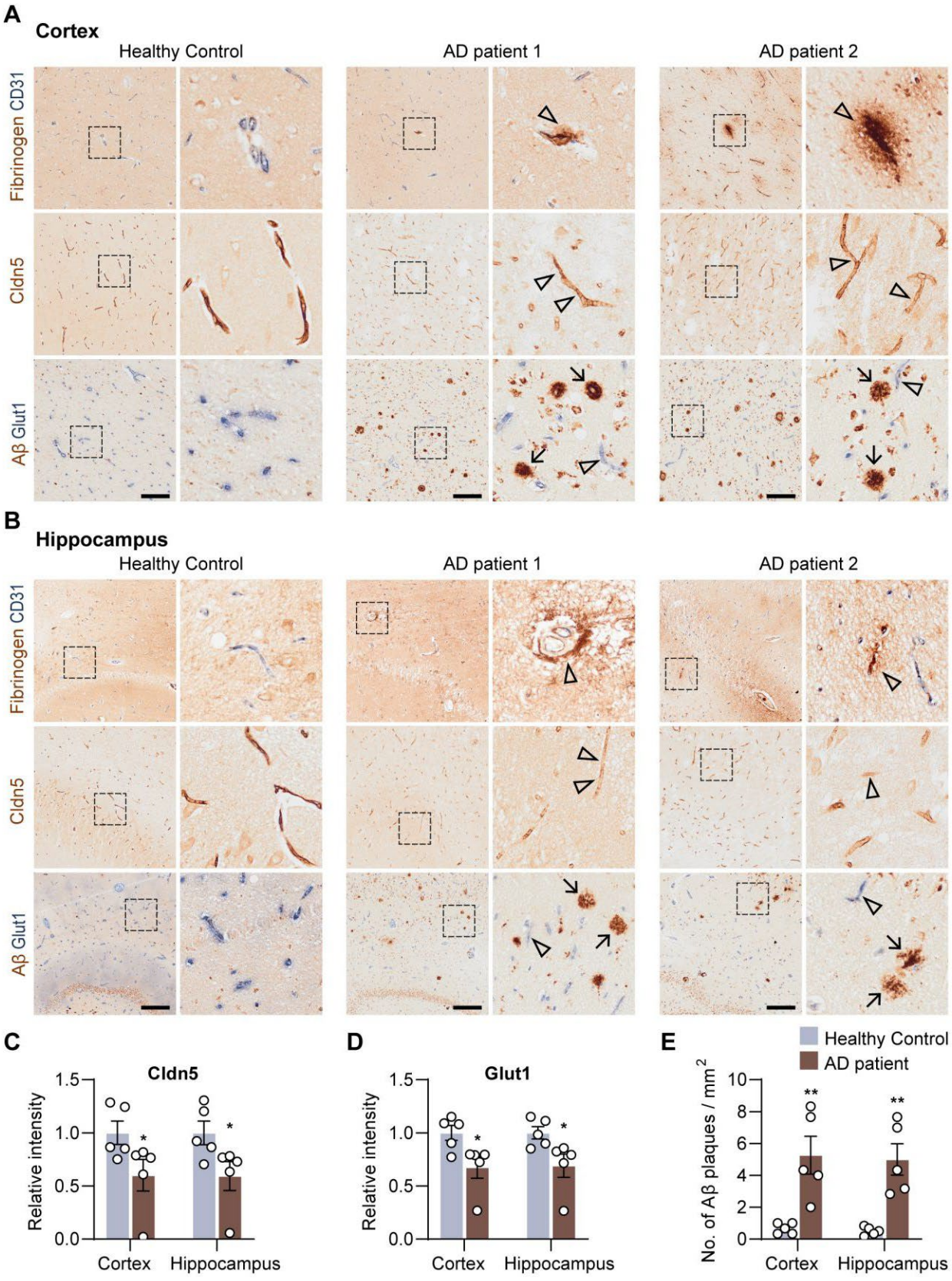

Figure 1
170x225 mm (x DPI)

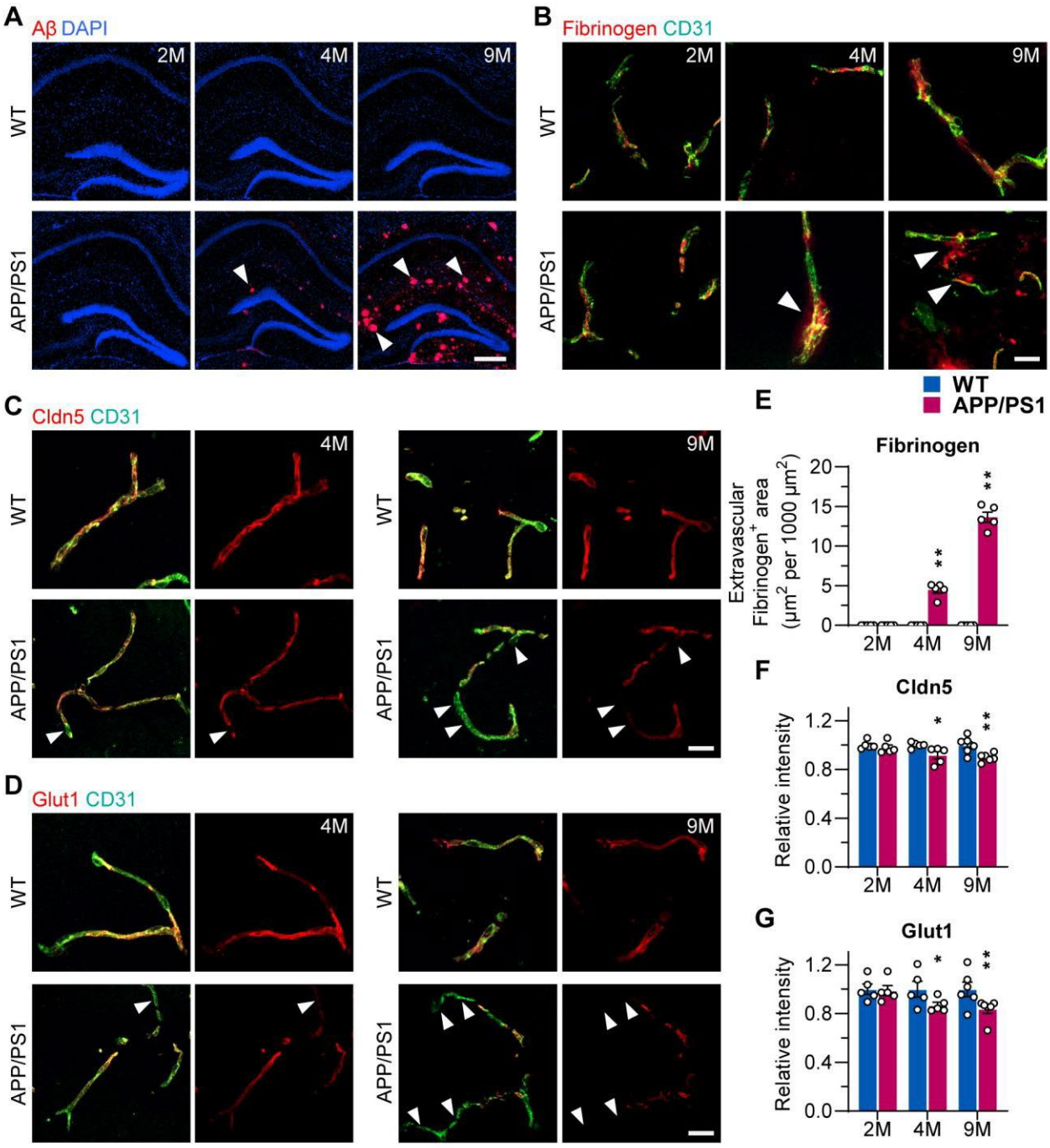

Figure 2
169x184 mm (x DPI)

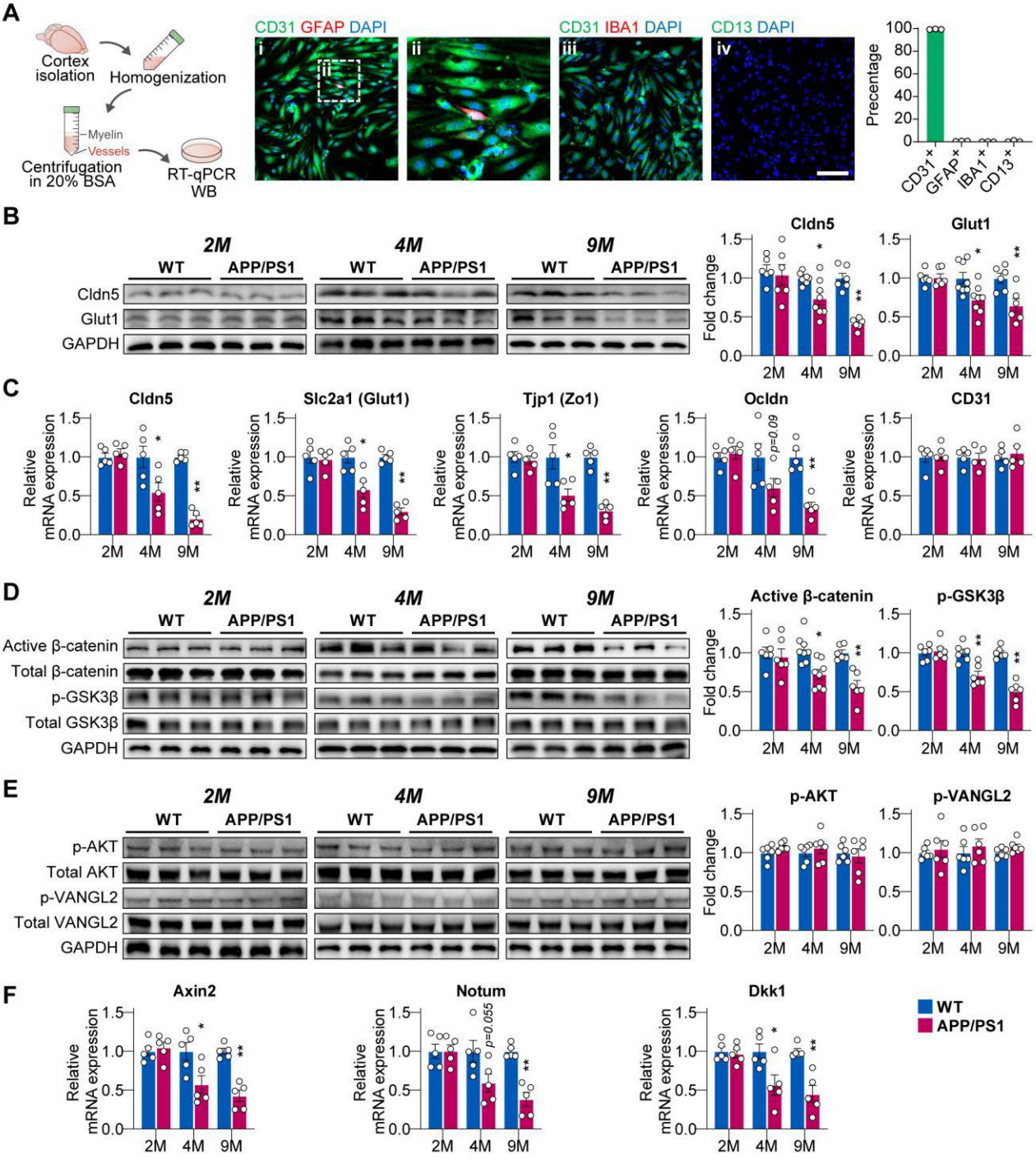

Figure 3
170x189 mm (x DPI)

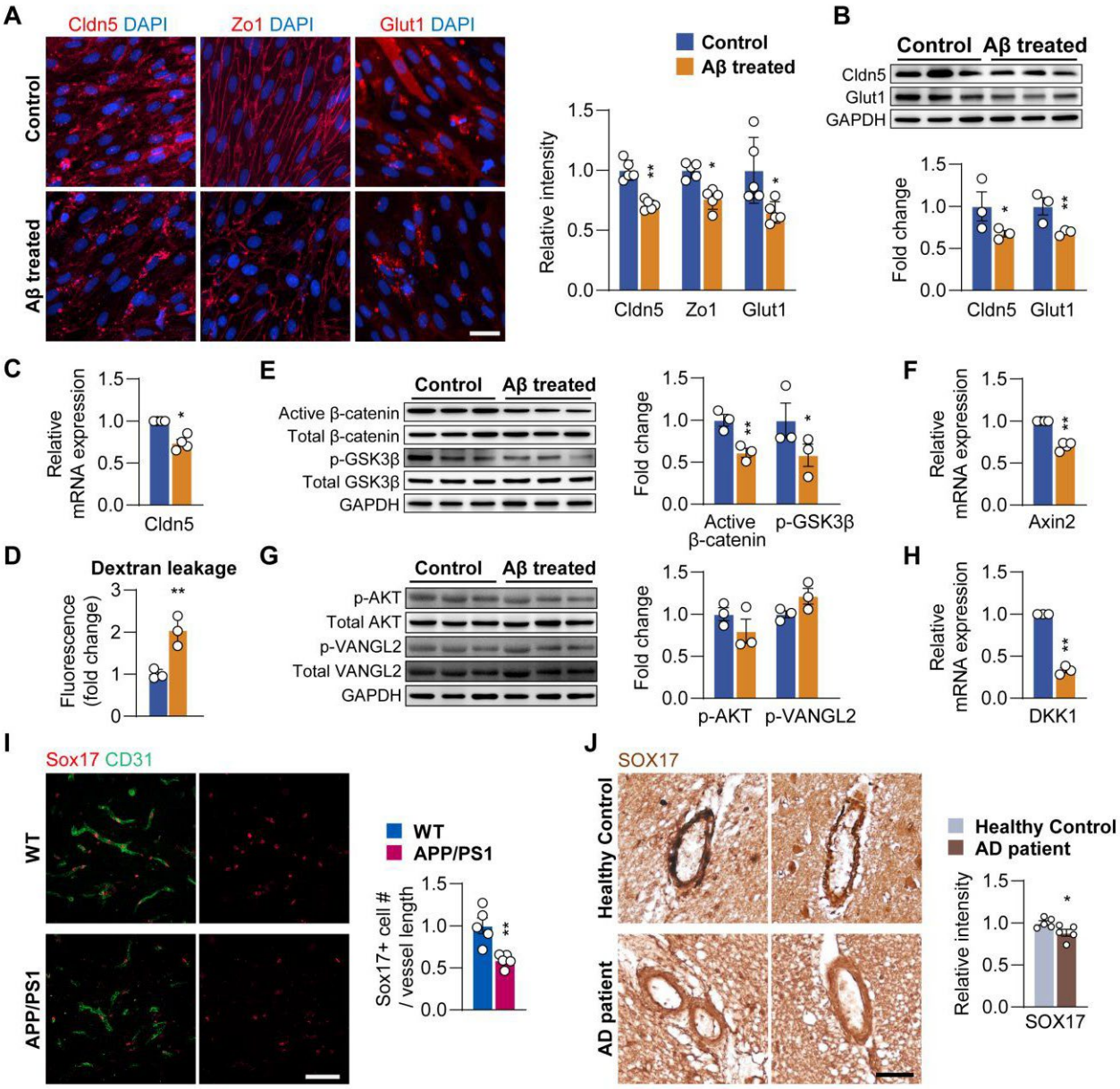

Figure 4
170x166 mm (x DPI)

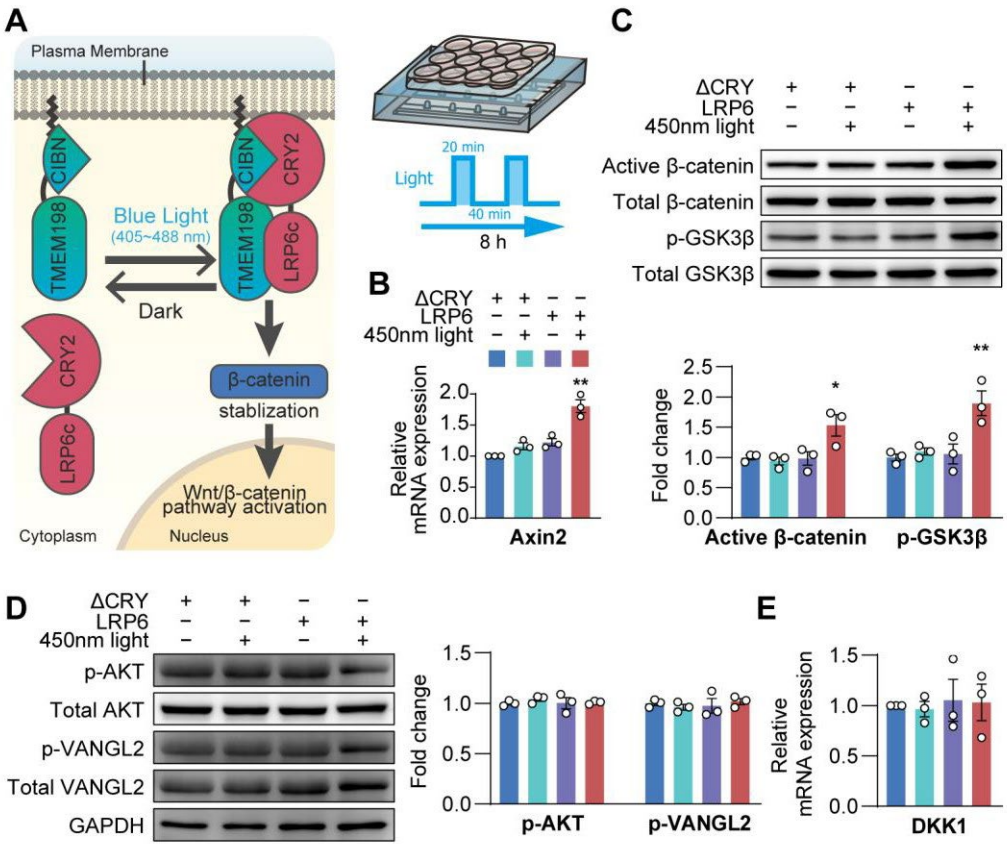

Figure 5
138x115 mm (x DPI)

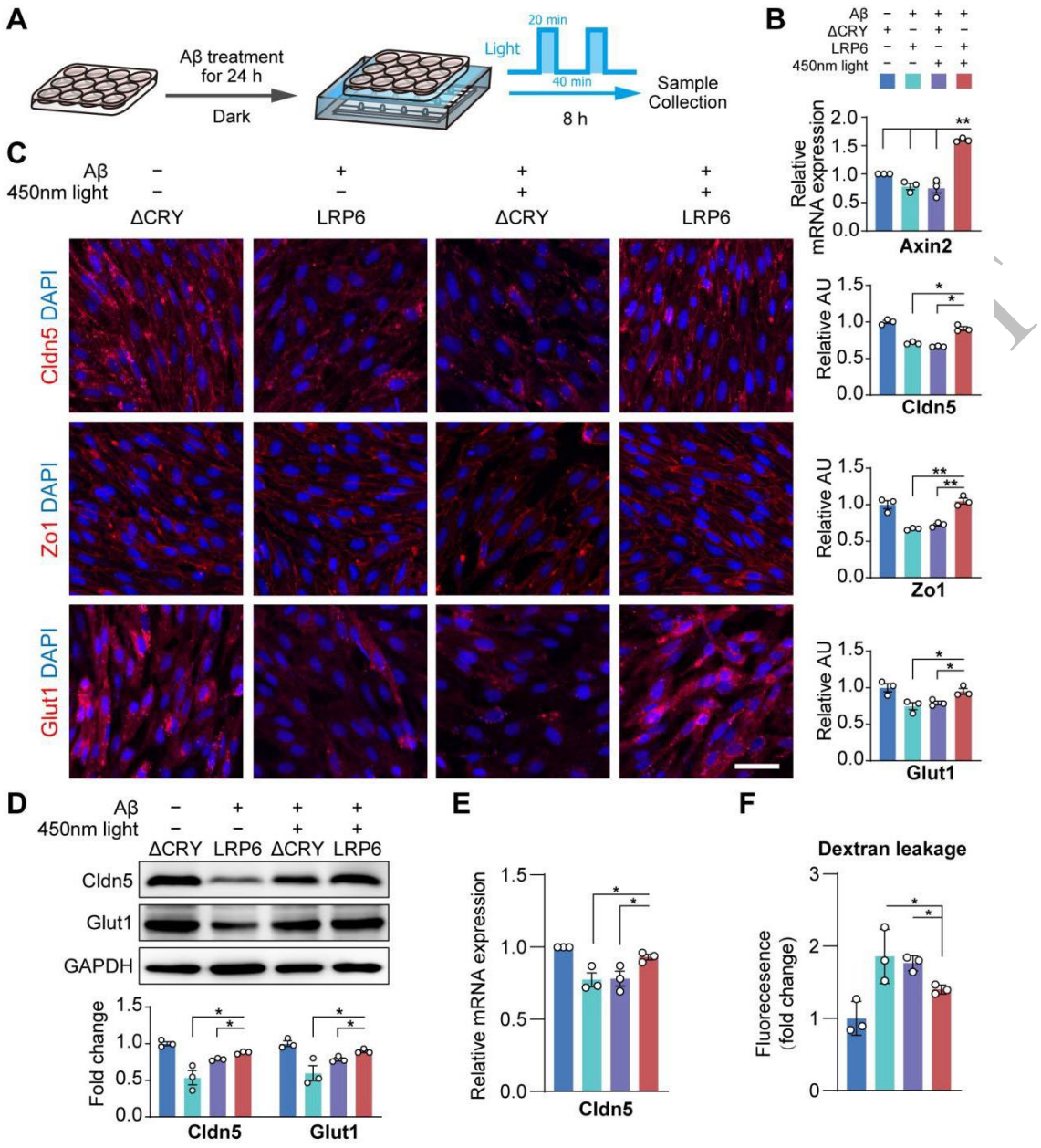

Figure 6
144x168 mm (x DPI)

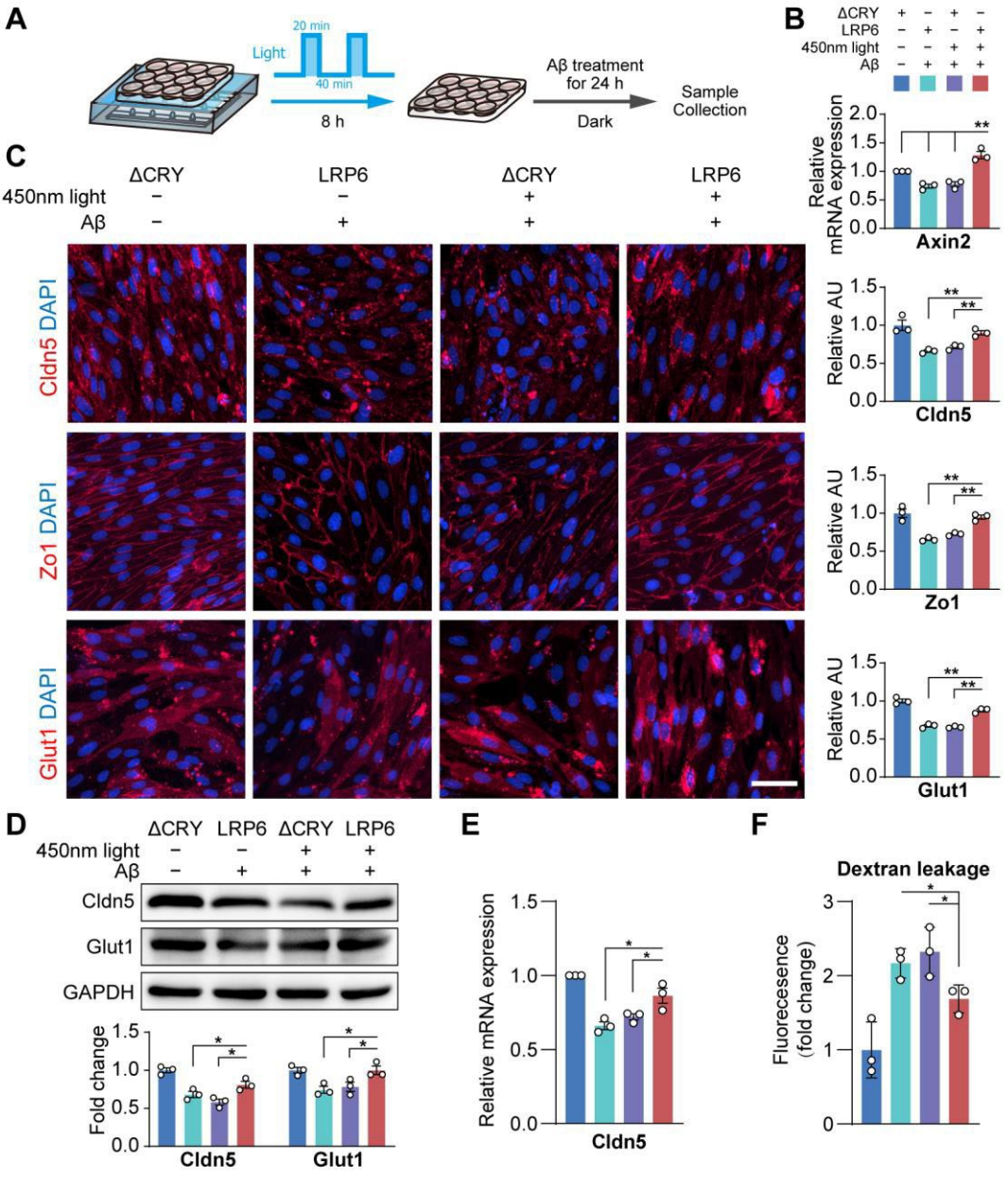

Figure 7
144x168 mm (x DPI)

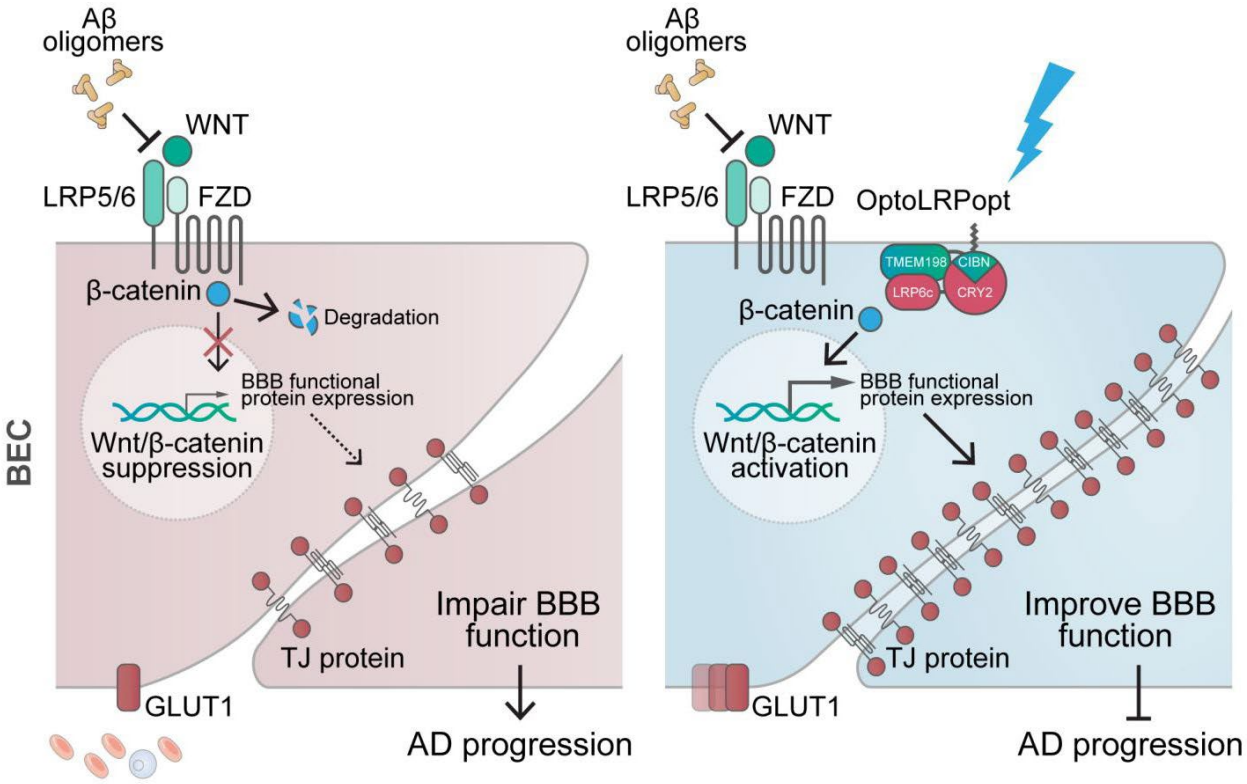

Figure 8
144x168 mm (x DPI)